

**UNCERTAINTIES INDUCED BY MULTIPLE
SCATTERING IN UPSTREAM DETECTORS
OF THE DIRAC SETUP**
(Part I: Vertex Position Uncertainty)

M.Pentia, S.Constantinescu

National Institute for Physics and Nuclear Engineering, Bucharest, P.O.Box MG-6,
RO-76900, ROMANIA.

Abstract

A statistical treatment of the Multiple Scattering (MS) in upstream detector tracking system of the DIRAC setup is done. The analytical dependence of the vertex position uncertainty $\sigma_{xy}^{(vertex)}$ on the coordinate error matrix, including MS correlated uncertainties and individual detector resolution, has been used to study some possible configurations of the upstream detector tracking system. It is discussed a background rejection method using track reconstructed vertex point position uncertainty.

Contents

1	Introduction	3
2	The particle track position errors due to multiple scattering	4
3	Track reconstruction parameters and their errors	5
4	Vertex position uncertainty	6
5	Analysis of some possible configurations	8
6	Conclusion	9

1 Introduction

In the present work we are studying the particle transport within upstream detector tracking system of the DIRAC setup (Figure 1). In this experiment the errors induced on the particle track due to MS in the upstream detector elements need to be carefully studied, especially if we try to find the track origin, the double track separation, the close opening angle and the relative momentum.

In this first paper we studied the errors due to MS on the reconstructed vertex position and have estimated the target region extension where the tracks can come from. To separate the good and background tracks coming from

the target, it is necessary to select a detector configuration which permits to minimize the extension of this region, in other words to minimize the uncertainty in the reconstructed vertex point position.

Using a linear track reconstruction procedure, with a nondiagonal error matrix, we expressed the track parameters and their errors. In such a way it was possible to study the propagation of coordinate errors to the vertex position uncertainty. The calculations have been done for the present day coordinate detector system configuration (see Figure 1) and also for some combinations of SciFi, MSGC and Si detectors.

The propagation of coordinate errors leads, for example, to a vertex position uncertainty which could be minimized by a proper tracking configuration.

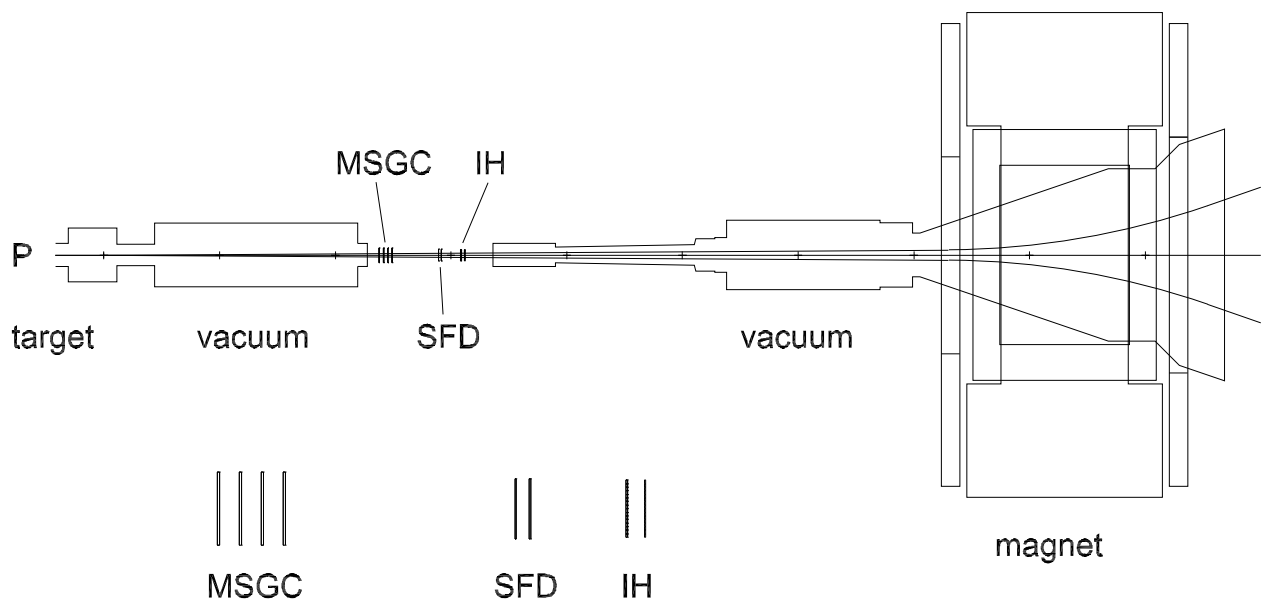


Figure 1:

2 The particle track position errors due to multiple scattering

When a charged particle is crossing the detector elements of a tracking system, it is subject to small deviations of the track due to MS. The effect is usually described by the theory of Molière (see for example Ref. [1]), which shows that, by crossing the detector material, thickness s , the particle is subject to successive small-angle deflections, symmetrically distributed around the incident direction. Applying the central limit theorem of statistics to a large number of independent scattering events, the Molière distribution of the scattering angle can be approximated by a Gaussian one [2]. It is sufficient for many applications to use Gaussian approximation for the central 98% of the plan projected angular distribution. The width of this distribution is the root mean square of the scattering angle [4]

$$\theta_0 = \frac{13.6 \text{ MeV}}{p\beta c} z_c \sqrt{\frac{s}{X_L}} \left[1 + 0.038 \ln \left(\frac{s}{X_L} \right) \right] \quad (1)$$

where $p, \beta c$ and z_c are the momentum, velocity and charge number of the incident particle, and X_L is the radiation length of the scattering medium. That is, the plan projected angle $\theta_{plane,x}$ or $\theta_{plane,y}$ of the deflection angle θ , onto the xOz and yOz planes, show an approximately Gaussian angular distribution.

$$\frac{1}{\sqrt{2\pi}\theta_0} \exp \left[-\frac{\theta_{plane}^2}{2\theta_0^2} \right] d\theta_{plane} \quad (2)$$

Deflections into $\theta_{plane,x}$ and $\theta_{plane,y}$ are independent, identically distributed, and

$$\theta_{space}^2 = \theta_{plane,x}^2 + \theta_{plane,y}^2.$$

The angular distribution is translated to a coordinate distribution by particle fly onto each detector plane (see Figure 2), and the more the intersected planes are the larger the distribution width (see Figure 3). The coordinate distribution is defined by statistical spread due to MS, and depends on the number and position of the intersected detector elements (see Table 1). It has the same form as angular distribution

$$\frac{1}{\sqrt{2\pi}\sigma_{x_i}} \exp \left[-\frac{x_i^2}{2\sigma_{x_i}^2} \right] dx_i \quad (3)$$

with the mean square deviation (distribution width) equals to the squares sum of the $(i-1)$ preceding distribution widths projected onto the i -th detector plane

$$\sigma_{x_i}^2 = \sum_{k=1}^{i-1} \theta_{0k}^2 (z_i - z_k)^2 \quad (4)$$

σ_{x_i} assigns the track position error measured on the i -th detector plane. In Figure 2 the scatter-plot and in Figure 3 the plan projected distribution of the x -coordinate points on the first four detector planes (MSGC) in the DIRAC setup are presented for 2000 MeV/c pions.

MS produces errors correlated between one layer and the following ones. Obviously a scattering in layer 1 produces correlated position errors in layers 3, 4 and so on. The proper error matrix is non-diagonal [5, 6]. The elements of this matrix are [6]

$$V_{ij} = \sum_{k=1}^{i-1} \theta_{0k}^2 (z_i - z_k) (z_j - z_k) \quad (5)$$

The uncorrelated position errors (detector resolution) σ_{ii}^{det} have to be added in squares in the diagonal terms of the error matrix V .

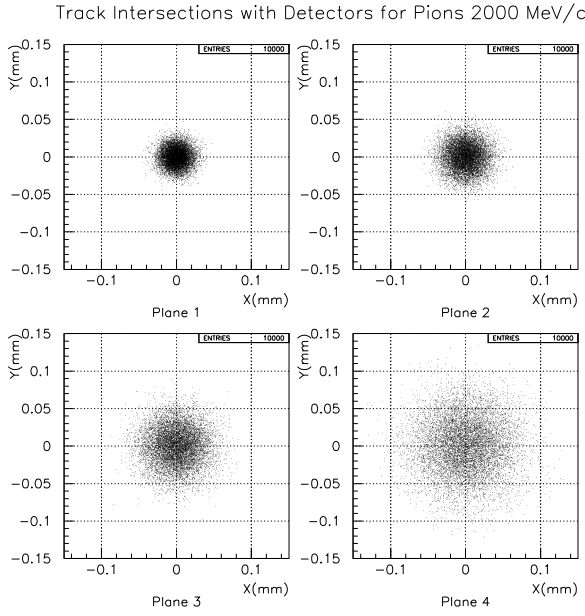


Figure 2: The track intersection pattern on the four MSGC detector planes, produced by MS in the material before every detector plane.

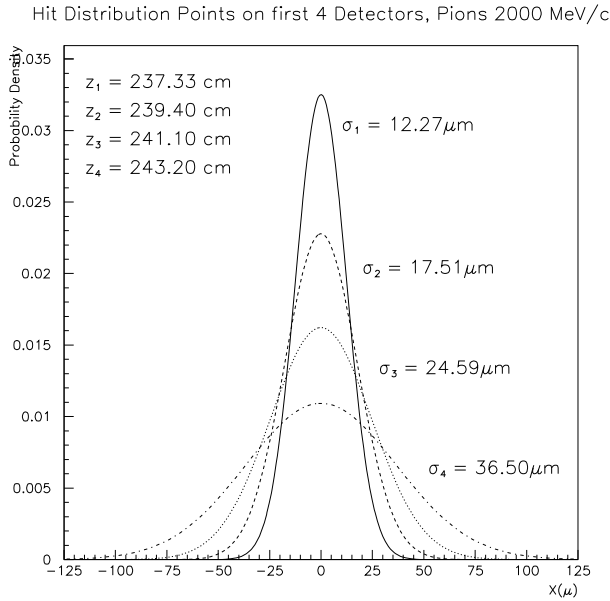


Figure 3: x -projection distribution of the track intersections with the 4 MSGC detector planes, produced by multiple scattering.

3 Track reconstruction parameters and their errors

The possibility to do an independent description of the MS data on x and y axis, allow a separate fitting by a linear relation

$$\begin{aligned} x &= x_0 + \alpha_x z \\ y &= y_0 + \alpha_y z \end{aligned} \quad (6)$$

With the coordinate and error data $(x_i \pm \sigma_{x_i})$, $(y_i \pm \sigma_{y_i})$, z_i , together with the corresponding error matrix V_{ij} as input data, it is possible to use the least squares procedure. For x -data set, the χ^2 in the matrix form is [6]

$$\chi^2 = (X - HA_x)^T V^{-1} (X - HA_x) \quad (7)$$

where

$$X = \begin{pmatrix} x_1 \\ x_2 \\ \vdots \\ x_n \end{pmatrix}; H = \begin{pmatrix} 1 & z_1 \\ 1 & z_2 \\ \vdots & \vdots \\ 1 & z_n \end{pmatrix}; A_x = \begin{pmatrix} x_0 \\ \alpha_x \end{pmatrix} \quad (8)$$

Then the least squares criterion imposes

$$\frac{\partial \chi^2}{\partial A_x} = 0 \quad \text{or} \quad H^T V^{-1} (X - HA_x) = 0 \quad (9)$$

By solving the linear system with respect to A_x we get the fit parameters

$$A_x = \begin{pmatrix} x_0 \\ \alpha_x \end{pmatrix} = (H^T V^{-1} H)^{-1} (H^T V^{-1} X) \quad (10)$$

and the error of these parameters

$$E_{A_x} = \begin{pmatrix} \sigma_{x_0}^2 & \sigma_{x_0} \sigma_{\alpha_x} \\ \sigma_{\alpha_x} \sigma_{x_0} & \sigma_{\alpha_x}^2 \end{pmatrix} = (H^T V^{-1} H)^{-1} \quad (11)$$

It must be pointed out that the track reconstructed parameter errors (11) do not depend

on the particular track coordinate values (x_i, y_i) , the errors depend only on the z_i layer position and on the θ_{0i} mean scattering values, of the H and V matrices.

We applied the same procedure for y coordinate, in order to find the best fit parameters and their errors. Immediately we have the x and y vertex coordinate

$$(x_0 \pm \sigma_{x_0}, y_0 \pm \sigma_{y_0}) \quad (12)$$

and the $\sigma_{xy}^{(vertex)}$ vertex position uncertainty

$$\sigma_{xy}^{(vertex)} = \sqrt{\sigma_{x_0}^2 + \sigma_{y_0}^2} \quad (13)$$

Because $\sigma_{x_0} = \sigma_{y_0}$, then $\sigma_{xy}^{(vertex)} = \sqrt{2}\sigma_{x_0}$, and represents the mean radius of the reconstructed vertex pattern on the target plane. It depends exclusively on the tracking configuration (z_i detector positions) and on MS strength (θ_{0i}).

4 Vertex position uncertainty

With the track reconstruction procedure described earlier, we could evaluate the vertex position resolution (uncertainty) $\sigma_{xy}^{(vertex)}$ (13) by means of the $\sigma_{x_0}^2$ value as the first element of the E_{A_x} matrix (11) of the track parameter errors.

For MS evaluation we had in view all the materials in the present day DIRAC configuration (see Figure 1), in the space between target and magnet. They are presented in Table 1.

A Monte-Carlo study of the particle transport within upstream part of the detector system has been done. The track reconstruction vertex points distribution are presented in Figure 4.

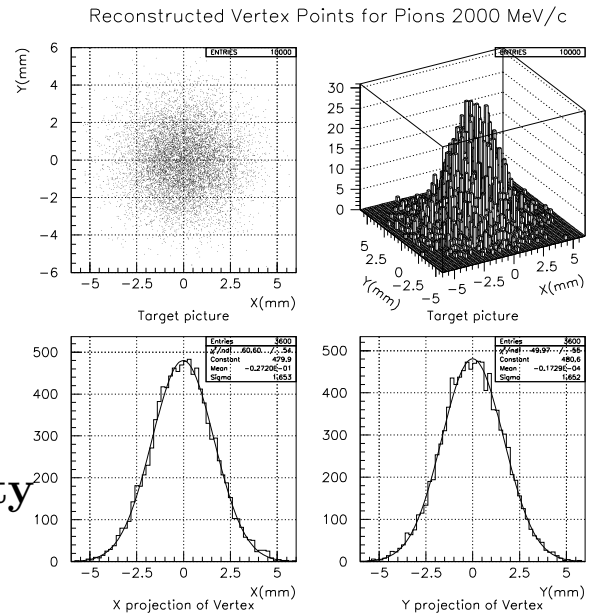


Figure 4:

Table 1.

Ndet	Detector material	z position (cm)	Thickness (μm)	XL (cm)	θ_0 plane (mrad)	Detector resolution (μm)	MS resolution (μm)
1	Mylar	229	250	28.7	0.14732	-	0.0
2	MSGC0	237.3	6500	116.0	0.40974	40	12.27
3	MSGC1	239.4	6500	116.0	0.40974	40	17.51
4	MSGC2	241.1	6500	116.0	0.40974	40	24.59
5	MSGC3	243.2	6500	116.0	0.40974	40	36.50
6	SciFi	287.78	2500	42.4	0.42132	125	399.34
7	SciFi	290.28	2500	42.4	0.42132	125	420.25
8	IH A	308.4	2000	42.4	0.37287	-	582.40
9	IH B	311.6	2000	42.4	0.37287	-	612.53
10	Mylar	334.4	250	28.7	0.14732	-	842.23

Table 2.

Ndet	$x(\mu m)$	$\sigma_{ii}^{det}(\mu m)$	$\sigma_{ii}^{MS}(\mu m)$	$y(\mu m)$	$\sigma_{ii}^{det}(\mu m)$	$\sigma_{ii}^{MS}(\mu m)$	$z(cm)$
1	0.000	-	0.000	0.000	-	0.000	229.00
2	6.665	40.0	12.272	-15.585	40.0	12.272	237.33
3	5.462	40.0	17.512	-13.247	40.0	17.512	239.40
4	1.155	40.0	24.594	3.708	40.0	24.594	241.10
5	-16.933	40.0	36.504	32.080	40.0	36.504	243.20
6	-486.698	125.0	399.337	960.363	125.0	399.337	287.78
7	-516.797	125.0	420.248	1016.788	125.0	420.248	290.28
8	-784.642	-	582.401	1429.043	-	582.401	308.40
9	-832.897	-	612.533	1490.921	-	612.533	311.60
10	-1200.304	-	842.229	1865.362	-	842.229	334.40

With given (measured) coordinates and associated errors (including intrinsic detector resolution σ_{ii}^{det} and MS error σ_{ii}^{MS}), as are given in Table 2, the track reconstruction procedure uses the symmetric nondiagonal correlation matrix, which for actual configuration looks as follows

$$\begin{pmatrix} .100E+01 & .000E+00 & .000E+00 & .000E+00 & .000E+00 & .000E+00 & .000E+00 & .000E+00 & .000E+00 & .000E+00 \\ .000E+00 & .100E+01 & .103E+00 & .111E+00 & .113E+00 & .607E-01 & .604E-01 & .343E-13 & .357E-13 & .455E-13 \\ .000E+00 & .103E+00 & .100E+01 & .197E+00 & .222E+00 & .169E+00 & .168E+00 & .976E-13 & .102E-12 & .132E-12 \\ .000E+00 & .111E+00 & .197E+00 & .100E+01 & .335E+00 & .311E+00 & .311E+00 & .182E-12 & .190E-12 & .248E-12 \\ .000E+00 & .113E+00 & .222E+00 & .335E+00 & .100E+01 & .508E+00 & .509E+00 & .300E-12 & .313E-12 & .409E-12 \\ .000E+00 & .607E-01 & .169E+00 & .311E+00 & .508E+00 & .100E+01 & .914E+00 & .545E-12 & .570E-12 & .751E-12 \\ .000E+00 & .604E-01 & .168E+00 & .311E+00 & .509E+00 & .914E+00 & .100E+01 & .549E-12 & .575E-12 & .759E-12 \\ .000E+00 & .343E-13 & .976E-13 & .182E-12 & .300E-12 & .545E-12 & .549E-12 & .100E+01 & .357E-24 & .481E-24 \\ .000E+00 & .357E-13 & .102E-12 & .190E-12 & .313E-12 & .570E-12 & .575E-12 & .357E-24 & .100E+01 & .508E-24 \\ .000E+00 & .455E-13 & .132E-12 & .248E-12 & .409E-12 & .751E-12 & .759E-12 & .481E-24 & .508E-24 & .100E+01 \end{pmatrix}$$

Finally the linear track reconstructed data are

$$\begin{aligned} x_0 &= 1973.896 \pm 1829.597 \mu m & ; & & \alpha_x &= -0.00082 \pm 0.00077 \\ y_0 &= -3944.988 \pm 1829.597 \mu m & ; & & \alpha_y &= 0.00164 \pm 0.00077 \end{aligned} \quad (14)$$

and the vertex position uncertainty, according to (13) and (14) is

$$\sigma_{xy}^{(vertex)} = 2587.4 \mu m$$

and represents the mean radius of the reconstructed vertex point pattern on the target plane, for 2000 MeV/c pions.

Vertex Position Uncertainty v.s. First Detector position – Pions 2000 MeV/c

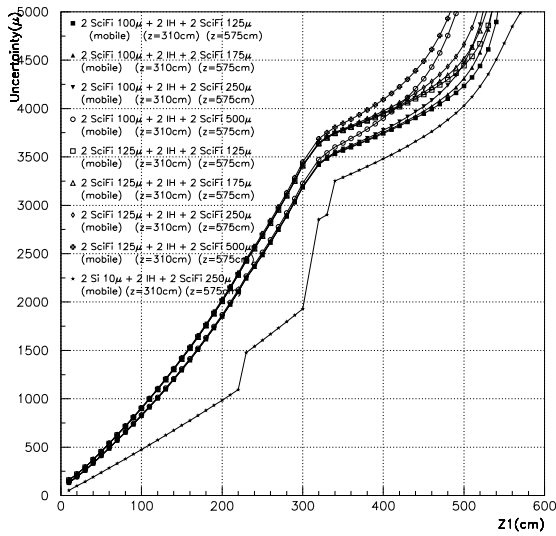


Figure 5: The track reconstruction configuration with 2 coordinate detector pairs, one moving, the other fixed.

5 Analysis of some possible configurations

Our study has been focused on the dependence of the vertex position uncertainty $\sigma_{xy}^{(vertex)}$ on first detector pair position (z_1).

We took in this study two types of tracking systems. The first one with two pairs of SciFi coordinate detectors and the second one with three pairs of MSGC and SciFi detector pair combinations. In both of these cases we compared the results with a Si microstrip and SciFi combination.

The most affecting vertex resolution (uncertainty) is the closest to the target coordinate detector. As close this detector can be

Vertex Position Uncertainty v.s. First Detector position – Pions 2000 MeV/c

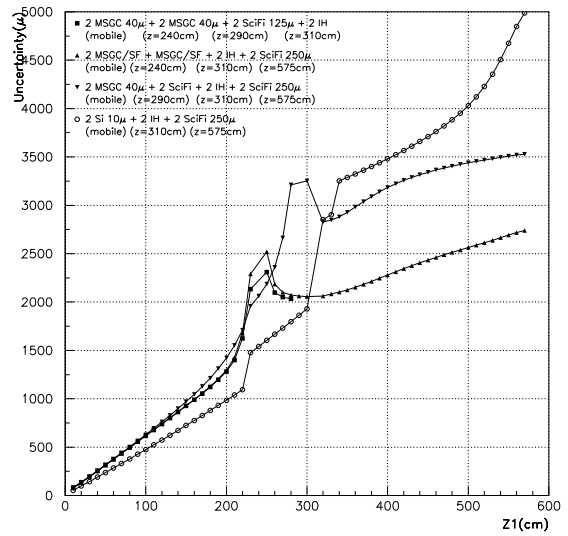


Figure 6: The track reconstruction configuration with 3 coordinate detector pairs, one moving and other two fixed. For comparison is presented the 2 detector pairs arrangement with Si & SciFi coordinate detectors.

placed, the best vertex position resolution can be obtained. This is why we studied the vertex position uncertainty as a function of the first detector position. In such a way we considered the first detector pair as a moving one and are looking for the vertex position uncertainty variation. The last detector pair in both of the cases have been considered a SciFi placed right before the magnet (about 6 m from the target). The results are presented in Figure 5 and Figure 6.

In Figure 5 there are presented a lot of combination of SciFi detector pairs. The first pair (moving) are $100\mu\text{m}$ and $125\mu\text{m}$ intrinsic resolution as long as the last one are $125\mu\text{m}$, $175\mu\text{m}$, $250\mu\text{m}$ and $500\mu\text{m}$. All other elements in the upstream channel have been included in the particle transport study. They are the mylar foils and Ionisation Hodoscopes (IH) as are presented in the Table 1. From

Figure 5 it can be seen that there are a small difference between all kind of SciFi combinations. Nevertheless, they are separated in 2 groups, one with 100 μm and the other with 125 μm as moving coordinate detector pair. For all of them the vertex resolution varies uniformly with increasing z_1 distance between moving detector and the target. When z_1 becomes greater than 310 cm (the moving detector passes the IH's, the most important scatterer) and closes to the fixed SciFi pair, the vertex resolution becomes worse.

In the same Figure 5 it can be seen the vertex resolution variation for a silicon microstrip detector pair (10 μm coordinate resolution). This one is very sensitive to any changement in the scattering environment. At about $z_1 = 240$ cm, it "sees" the changement in the scattering due to first mylar foil. The same changement is seen at about $z_1 = 310$ cm, position of IH's, and at about $z_1 = 335$ cm, position of the second mylar foil.

The SciFi detectors do not "see" the passage through the mylar foil, because their intrinsic resolution ($\approx 100\mu m$) is larger than the MS resolution contribution of the mylar, and they are added in squares.

In Figure 6 there is a more complicated variation of the vertex position resolution. Here we considered three coordinate detector pairs. In this case the vertex resolution do not shows a so large variation as in previous case. This is due to the fact that three detector pairs now keep the linear track in a more rigide situation. Nevertheless, when the moving detector becomes closer to a fixed one, the vertex resolution increases very large. This is due to the fact that the "error bar" constrains (detector resolution) of the two closest detectors becomes very permissibile for reconstructed tracks.

In the case of MSGC/SciFi combination, the moving detector pair shows a large transparence for reconstructed tracks at about $z_1 = 240$ cm, when it meets the second MSGC/SciFi coordinate detector pair. The same effect is present in the case of moving MSGC pair through the second coordinate detector pair (SciFi) at about $z_1 = 290$ cm. After passing the second coordinate detector pair, the vertex resolution is not so affected, because now the closest coordinate detector pair relative to target, is another one, the first fixed pair.

In the Figure 6 is presented also the same combination of silicon microstrip detector as in Figure 5. Here it can be seen that even the silicon detector in a two pair combination can present a worse vertex position resolution than a three pair MSGC-SciFi combination.

6 Conclusion

For the background and good particle track separation it is possible to identify the track intersection points with the target plane, and so to find the source coordinates (vertex position) of the detected particles. After track reconstruction within the present day tracking detector system the pointlike source for pions 2000 MeV/c, becomes, due to MS, a spot of mean radius 2587 μm . Within the domain specified by this radius there is not possible to separate the background and good particle tracks, but for outside this region, the background can easely be rejected.

The present paper shows the possibilities to reduce the reconstructed vertex point spread for interesting particles, using a proper tracking detector configuration for the upstream DIRAC setup.

References

- [1] W.T. Scott, Rev. Mod. Phys. 35 (1963) 231.
- [2] A. Klatchko, B.C.Choudhary and T. Huehn, Estimation of the Multiple Coulomb Scattering Error for Various Numbers of Radiation Lengths, Fermilab-Pub-92/289 (1992).
- [3] G.R. Lynch and O.I. Dahl, Nucl. Instr. and Meth. B 58 (1991) 6.
- [4] D.E.Groom et al, Particle Data Group, Eur.Phys.J. C15, 1 (2000)
- [5] E.J. Wolin and L.L. Ho, Nucl. Instr. and Meth. A 329 (1993) 493.
- [6] M. Pentia, R. Muresan, A.G. Litvinenko, Nucl. Instr. and Meth. A 369 (1996) 101.
- [7] P.R. Bevington, Data Reduction and Error Analysis for the Physical Sciences (McGraw-Hill, New York, 1969).